ELSEVIER

Journal of Hazardous Materials A137 (2006) 734–741

Journal of Hazardous Materials

www.elsevier.com/locate/jhazmat

Characteristic overpressure–impulse–distance curves for vapour cloud explosions using the TNO Multi-Energy model

Fernando Díaz Alonso [a,*], Enrique González Ferradás [a], Juan Francisco Sánchez Pérez [a], Agustín Miñana Aznar [a], José Ruiz Gimeno [a], Jesús Martínez Alonso [b]

[a] *Grupo de Investigación "Seguridad e Higiene en la Industria", Departamento de Ingeniería Química, Universidad de Murcia, Campus Universitario de Espinardo, 30100 Murcia, Spain*

[b] *Unidad de Protección Civil, Delegación del Gobierno en Madrid, C/García Paredes, 65. 28010 Madrid, Spain*

Received 20 February 2006; received in revised form 28 March 2006; accepted 1 April 2006
Available online 18 April 2006

Abstract

A number of models have been proposed to calculate overpressure and impulse from accidental industrial explosions. When the blast is produced by ignition of a vapour cloud, the TNO Multi-Energy model is widely used. From the curves given by this model, data are fitted to obtain equations showing the relationship between overpressure, impulse and distance. These equations, referred herein as *characteristic* curves, can be fitted by means of power equations, which depend on explosion energy and charge strength. *Characteristic* curves allow the determination of overpressure and impulse at each distance.

Keywords: Vapour cloud explosion; Overpressure; Impulse; TNO Multi-energy model; Industrial accident

1. Introduction

Vapour cloud explosions (VCEs) are serious hazards in refining and petrochemical industries [1]. Since the 1970s, when several devastating vapour cloud explosions occurred, a considerable degree of attention and research effort has been focussed on this subject [2]. A number of examples of VCE accidents can be found in the literature [3,4], amongst them the Flixborough explosion of June 1, 1974, which was especially destructive. It was caused by the uncontrolled leakage of about 30 tons of cyclohexane at the Nypro plant in Flixborough, UK. A few minutes after the leakage started, the cyclohexane cloud ignited and a violent explosion occurred, causing the death of 28 men and severe damage to on-site infrastructure [5]. Another serious industrial accident occurred at Beek in The Netherlands on November 7, 1975, when a violent VCE occurred within a naphta-cracker installation. The explosion resulted in several fatalities, destroyed the installation and resulted in severe damage to the immediate surroundings with window breakage up to 4.5 km from the source [6]. Apart from these two examples, many other VCEs have occurred and, unfortunately, these types of devastating accidents still happen. Regarding the magnitude of an explosion, the two most important and dangerous factors are overpressure and impulse (the latter depending on overpressure and positive phase time duration), which are chiefly responsible for injury to humans, and structural and environmental damage. Table 1 shows some damages for different overpressures and impulses.

To assess damage, models are necessary to calculate the magnitude of an explosion as a function of distance from the centre. Furthermore, with proper safety guidelines, appropriate structural design and safe distance considerations, blast hazards from VCEs could be reduced to acceptable levels [1].

For vapour cloud explosions, the TNO Multi-Energy model is often used to determine overpressure and positive phase duration time as a function of distance [7]. Lees [3] makes reference to this method in his textbook. The Multi-Energy concept is based on the observation that the explosive potential of a vapour cloud is primarily determined by the obstructed and/or partially confined parts of the cloud [8]. Some data have been obtained and

* Corresponding author at: Departamento de Ingeniería Química, Facultad de Química, Universidad de Murcia, Campus Universitario de Espinardo, 30100 Murcia, Spain. Tel.: +34 968 36 39 37/34 968 36 39 36; fax: +34 968 36 41 48.
E-mail address: ferdiaz@um.es (F.D. Alonso).

0304-3894/$ – see front matter © 2006 Elsevier B.V. All rights reserved.
doi:10.1016/j.jhazmat.2006.04.005

Nomenclature

a	parameter used in fitted scaled overpressure equation – Eq. (8)
b	exponent of the fitted scaled overpressure equation – Eq. (8)
c	parameter used in fitted scaled impulse equation – Eq. (9)
c_0	sound velocity in air (340 m/s)
d	exponent of the fitted scaled impulse equation – Eq. (9)
E_{exp}	explosion energy (J)
i	impulse (Pa s)
i'	scaled impulse (dimensionless)
K	constant overpressure value from Eq. (10) (Pa).
P_s	side-on overpressure (Pa)
P_0	atmospheric pressure (Pa)
P'	scaled overpressure (dimensionless)
R'	scaled distance (dimensionless)
t_p	positive phase duration time (s)
t'_p	scaled positive phase duration time (dimensionless)
z	distance to the explosion's centre (m)

Greek symbols

α	parameter used in characteristic equation – Eq. (11)
β	exponent of the characteristic equation – Eq. (11)

analysed from explosion experiments [9,10] and several authors have proposed methodologies to select the appropriate charge strength [11–14]. The Multi-Energy model is widely used for consequence analysis [15–19], also for domino hazards [20].

This model uses the following parameters:

$$P' = \frac{P_s}{P_0} \tag{1}$$

$$R' = \frac{z}{(E_{exp}/P_0)^{1/3}} \tag{2}$$

$$t_p = \frac{t'_p (E_{exp}/P_0)^{1/3}}{c_0} \tag{3}$$

$$i = 1/2\ P_s\, t_p \tag{4}$$

where P' (dimensionless) is the scaled overpressure; P_s (Pa) is the side-on overpressure; P_0 (101 000 Pa) is atmospheric pressure; R' (dimensionless) is the scaled distance; z (m) is the distance from the explosion centre; c_0 (340 m/s) is sound velocity in air; i (Pa s) is the wave's impulse; t_p (s) is the positive phase duration time; t'_p (dimensionless) is the scaled positive phase duration time and E_{exp} (J) is the explosion energy.

The TNO Multi-Energy model does not solve the relationship between impulse and scaled distance. Since this relationship is necessary for the aim of this paper, Eqs. (1), (3) and (4) are combined to obtain:

$$i = 1/2(P_0^{2/3} E_{exp}^{1/3}/c_0) P'\, t'_p \tag{5}$$

A new dimensionless parameter called *scaled impulse* is defined, as follows:

$$i' = P'\, t'_p \tag{6}$$

and from Eq. (5), the following is obtained

$$i' = 2\left[\frac{c_0}{(P_0^{2/3} E_{exp}^{1/3})}\right] i \tag{7}$$

showing the relationship between impulse (i) and scaled impulse (i'). From each R' value (corresponding to each distance), the scaled impulse is calculated (Eq. (6)) using the TNO curves (Fig. 5.8A and C in [7]), and the curves in Fig. 1 are obtained.

2. *Characteristic* overpressure–impulse–distance curves for VCEs

For every explosion, it is possible to obtain the overpressure–impulse–distance relationship, called here the '*characteristic* curve'. Fig. 2 shows, graphically, the *characteristic curve*, traced from the overpressure–distance and impulse–distance shock-wave profiles (taken from Figs. 5.8A in [7] and 3, respectively). Distances to the explosion centre (z_1, z_2,..., z_n) can also be included to display all the information within the same diagram.

Table 1
Damages on humans and buildings produced by different overpressures and impulses [3]

	Effect		Ps (Pa)	i (Pa s)
Humans	Eardrum rupture	Threshold	34500	–
		50%	103000–138000	–
	Lung damage	Threshold	83000–103000	16600–21000
		Severe	255000	51000
	Lethality (lung haemorrhage)	Threshold	255000–359000	51000–72000
		50%	359000–497000	72000–99000
		100%	497000–690000	99000–138000
Buildings	Partially demolished	80%	35000	13000
	Moderated damage	25%	28000	11000
	Minor damage (repairable)	10%	12000	6000

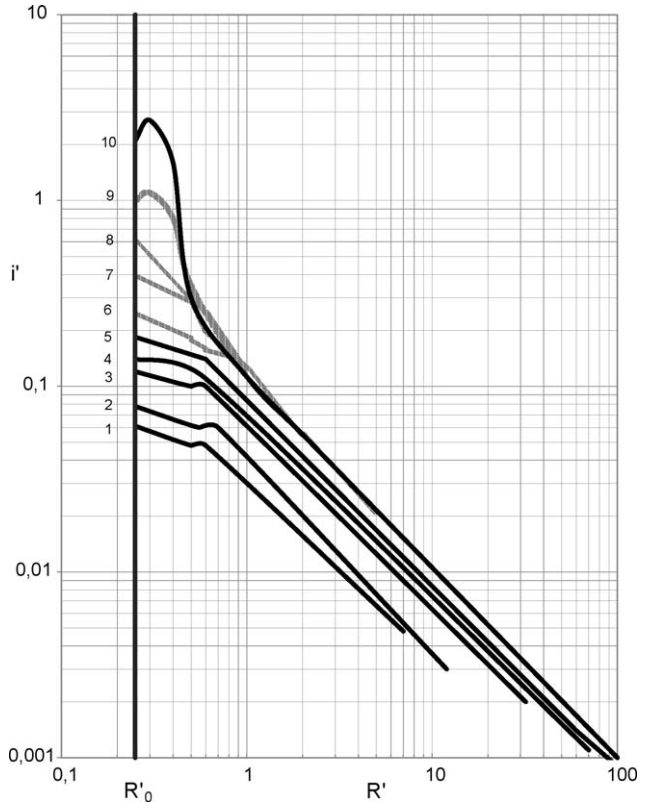

Fig. 1. Scaled impulse versus scaled distance for the Multi-Energy method.

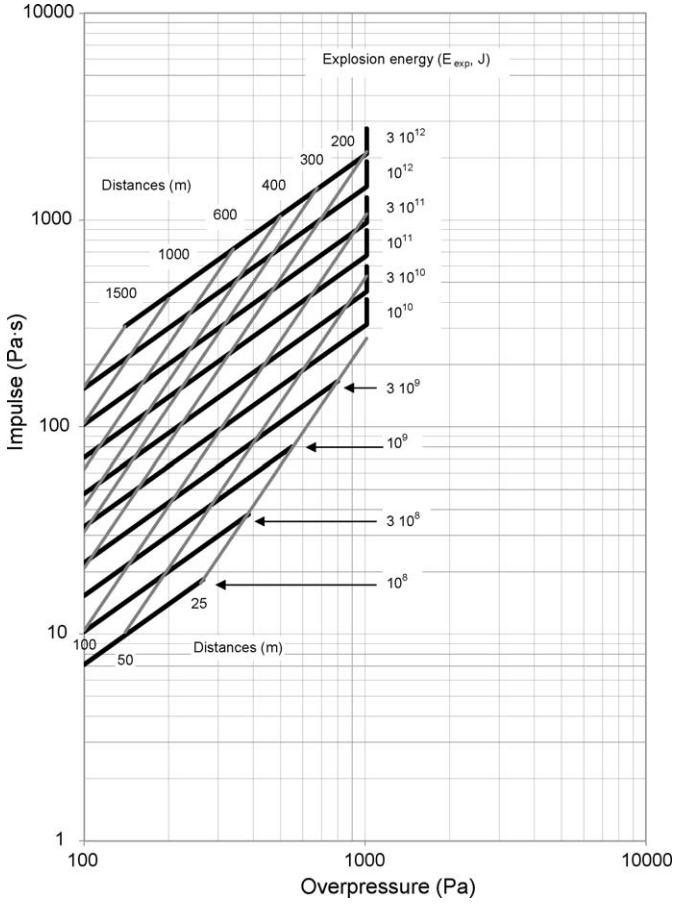

Fig. 3. *Characteristic* curves and *iso-distance* lines of VCEs with different energies and a charge strength of 1. Obtained using the TNO Multi-Energy model.

However, it is not necessary to draw overpressure and impulse profiles to obtain the characteristic curves, as they can also be obtained analytically. To perform this operation, the relationships P' versus R' and i' versus R' (from Fig.5.8A [7] and Fig. 1, respectively) are fitted using power equations. To obtain good correlations, each curve is divided into several intervals, that are selected to optimize the R-squared values (which are considered by the authors to be good enough when they are higher than 0.98). It means that each curve is successively divided into 1, 2, 3,. . ., n intervals until all their R-squared values are higher than 0.98. These equations have the following general form:

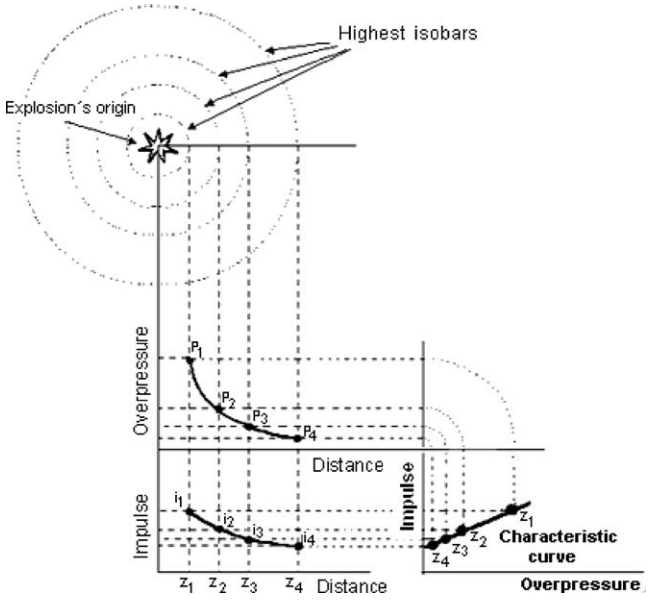

Fig. 2. Characteristic curve of an explosion: obtained from overpressure and impulse profiles.

For scaled overpressure : $P' = a\,R'^{b}$ (8)

For scaled impulse : $i' = c\,R'^{d}$ (9)

where a, b, c and d depend on charge strength and the selected interval. Tables 2 and 3 show the fitted equations for scaled overpressure scaled impulse, respectively.

3. Results and discussions

Depending on the interval and using Eqs. (1) and (7), the *characteristic* equations are obtained from the corresponding overpressure and impulse equations. They have the following general form:

for the first interval of every charge strength (except strength 10) :

$$P_s = K \quad (10)$$

Table 2
Fitted equations for scaled overpressure from Fig. 5.8A of [7]

Explosion level	Interval for R'	a	b	Interval for R'	a	b
1	$0.23 \le R' < 0.6$	10^{-2}	0	$0.6 \le R' \le 7$	6.40×10^{-3}	−0.97
2	$0.23 \le R' < 0.7$	2×10^{-2}	0	$0.7 \le R' \le 12$	1.32×10^{-2}	−0.98
3	$0.23 \le R' < 0.6$	5×10^{-2}	0	$0.6 \le R' \le 30$	6.05×10^{-2}	−0.99
4	$0.23 \le R' < 0.5$	10^{-1}	0	$0.5 \le R' \le 70$	6.44×10^{-2}	−0.99
5	$0.23 \le R' < 0.6$	2×10^{-1}	0	$0.6 \le R' \le 90$	1.17×10^{-1}	−0.99
6	$0.23 \le R' < 0.6$	5×10^{-1}	0	$0.6 \le R' \le 100$	3.01×10^{-1}	−1.11
7	$0.23 \le R' < 0.5$	1	0	$0.5 \le R' \le 100$	4.06×10^{-1}	−1.20
8	$0.23 \le R' < 0.5$	2	0	$0.5 \le R' < 1$	4.76×10^{-1}	−2.08
	$1 \le R' < 2$	4.67×10^{-1}	−1.58	$2 \le R' \le 100$	3.18×10^{-1}	−1.13
9	$0.23 \le R' < 0.35$	5	0	$0.35 \le R' < 1$	4.87×10^{-1}	−2.03
	$1 \le R' < 2$	4.67×10^{-1}	−1.58	$2 \le R' \le 100$	3.18×10^{-1}	−1.13
10	$0.23 \le R' < 1$	4.41×10^{-1}	−2.39	$1 \le R' < 2$	4.67×10^{-1}	−1.58
	$2 \le R' \le 100$	3.18×10^{-1}	−1.13			

Table 3
Fitted equations for scaled impulse from Fig. 1

Explosion level	Interval for R'	c	d	Interval for R'	c	d
1	$0.23 \le R' < 0.6$	4.41×10^{-2}	−0.20	$0.6 \le R' \le 7$	2.96×10^{-2}	−0.94
2	$0.23 \le R' < 0.7$	5.22×10^{-2}	−0.27	$0.7 \le R' \le 12$	4.03×10^{-2}	−1.05
3	$0.23 \le R' < 0.6$	8.74×10^{-2}	−0.20	$0.6 \le R' \le 30$	6.05×10^{-2}	−0.99
4	$0.23 \le R' < 0.5$	1.4×10^{-1}	0	$0.5 \le R' \le 70$	6.77×10^{-2}	−0.97
5	$0.23 \le R' < 0.6$	1.25×10^{-1}	−0.26	$0.6 \le R' \le 90$	8.46×10^{-2}	−1.00
6	$0.23 \le R' < 0.8$	1.28×10^{-1}	−0.45	$0.8 \le R' \le 100$	1.14×10^{-1}	−1.03
7	$0.23 \le R' < 0.6$	1.98×10^{-1}	−0.49	$0.6 \le R' \le 100$	1.14×10^{-1}	−1. 03
8	$0.23 \le R' < 0.6$	1.66×10^{-1}	−0.90	$0.6 \le R' \le 100$	1.14×10^{-1}	−1. 03
9	$0.23 \le R' < 0.3$	1.11	0.89	$0.3 \le R' < 0.4$	3.08×10^{-1}	−1.08
	$0.4 \le R' < 0.8$	8.08×10^{-2}	−2.26	$0.8 \le R' \le 100$	1.14×10^{-1}	−1.03
10	$0.23 \le R' < 0.3$	10.82	1.14	$0.3 \le R' < 0.4$	3.15×10^{-1}	−1.79
	$0.4 \le R' < 0.5$	1.30×10^{-3}	−7.52	$0.5 \le R' \le 100$	1.14×10^{-1}	−1.03

for the remaining intervals : $i = \alpha\, E_{\exp}^{1/3}\, P_s^{\beta}$ (11)

where α and β depend on the selected interval and charge strength. Table 4 shows the constant K values from Eq. (10), while α and β values (from Eq. (11)) are shown in Table 5.

It can be deduced from Eq. (11) that, for each interval, the relationship between overpressure and impulse depends only on released energy $E_{\exp}$ and charge strength. The greater the explosion energy for the same charge strength, the higher the impulse for the same overpressure. It can also be deduced from the characteristic equations that parameter β, which is the slope of the *characteristic* curve in a log–log diagram, is constant for each interval. This means that *characteristic* curves are parallel lines whose position depends on explosion energy. If the points corresponding to the same distance on different *characteristic* curves are joined, *iso-distance* lines are obtained. To obtain the equations of these *iso-distance* lines for each interval, the fitted overpressure equation for that interval is taken (Eq. (8)). From Eqs. (1) and (2), we have:

$$P_s = a\, P_0 \left[\frac{z}{(E_{\exp}/P_0)^{1/3}} \right] b \tag{12}$$

Finding $E_{\exp}^{1/3}$ from Eq. (12) and substituting it into the corresponding *characteristic* equation, we have:

$$i = \alpha\, P_0^{1/3} \left(\frac{a\, P_0}{P_s} \right)^{1/b} z\, P_s^{\beta} \tag{13}$$

If the distance z is set at a constant value, the relationship between overpressure and impulse for that distance

Table 4
K-values for Eq. (10)

Explosion level	Interval for R'	K (Pa)
1	$0.23 \le R' < 0.6$	1013
2	$0.23 \le R' < 0.7$	2030
3	$0.23 \le R' < 0.6$	5070
4	$0.23 \le R' < 0.5$	10130
5	$0.23 \le R' < 0.6$	20260
6	$0.23 \le R' < 0.6$	50650
7	$0.23 \le R' < 0.5$	101300
8	$0.23 \le R' < 0.5$	202600
9	$0.23 \le R' < 0.35$	506500

Table 5
α- and β-values for Eq. (11)

Explosion level	Interval for R'	α	β			
1	$0.6 \le R' \le 7$	1.76×10^{-4}	0.97			
2	$0.7 \le R' \le 12$	5.76×10^{-5}	1.07			
3	$0.6 \le R' \le 30$	5.24×10^{-5}	1.02			
4	$0.5 \le R' \le 70$	3.96×10^{-5}	0.98			
5	$0.6 \le R' \le 90$	2.07×10^{-5}	1.01	Interval for R'	α	β
6	$0.6 \le R' < 0.8$	1.14×10^{-1}	−1.03	$0.8 \le R' \le 100$	2.51×10^{-5}	0.93
7	$0.5 \le R' < 0.6$	8.24×10^{-3}	0.41	$0.6 \le R' \le 100$	3.99×10^{-5}	0.86
8	$0.5 \le R' < 0.6$	4.60×10^{-3}	0.43	$0.6 \le R' < 1$	1.59×10^{-3}	0.50
	$1 \le R' < 2$	3.26×10^{-4}	0.65	$2 \le R' \le 100$	2.83×10^{-5}	0.91
9	$0.35 \le R' < 0.4$	3.13×10^{-3}	0.53	$0.4 \le R' < 0.8$	1.54×10^{-6}	1.11
	$0.8 \le R' < 1$	1.51×10^{-3}	0.51	$1 \le R' < 2$	3.26×10^{-4}	0.65
	$2 \le R' \le 100$	2.83×10^{-5}	0.91			
10	$0.23 \le R' < 0.3$	5.71×10^{3}	−0.48	$0.3 \le R' < 0.4$	3.31×10^{-4}	0.75
	$0.4 \le R' < 0.5$	9.70×10^{-18}	3.15	$0.5 \le R' < 1$	3.61×10^{-3}	0.43
	$1 \le R' < 2$	3.26×10^{-4}	0.65	$2 \le R' < 100$	2.83×10^{-5}	0.91

is obtained, which is the *iso-distance* equation. Introducing the constant values (a, b, α and β) for each interval, plotting the *characteristic* curves for different E_{exp} values (black lines) in the same diagram and tracing the lines that join the same distances (*iso-distances*, represented by grey lines), the curves in Figs. 3–12 are obtained (one for each charge strength). These plots allow a quick and simple determination of overpressure and impulse at each distance for an explosion whose energy and charge strength are known.

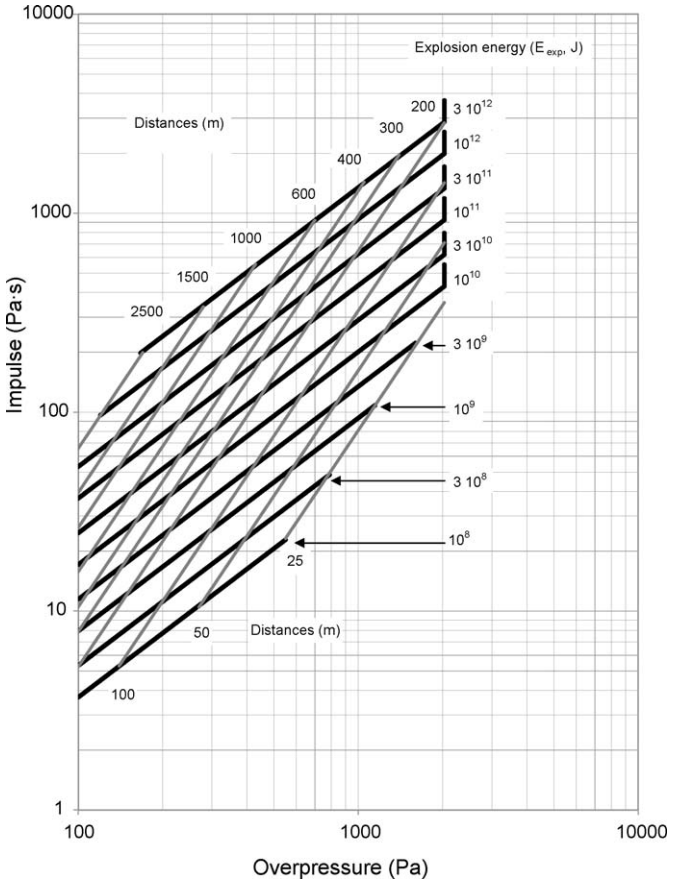

Fig. 4. *Characteristic* curves and *iso-distance* lines of VCEs with different energies and a charge strength of 2. Obtained using the TNO Multi-Energy model.

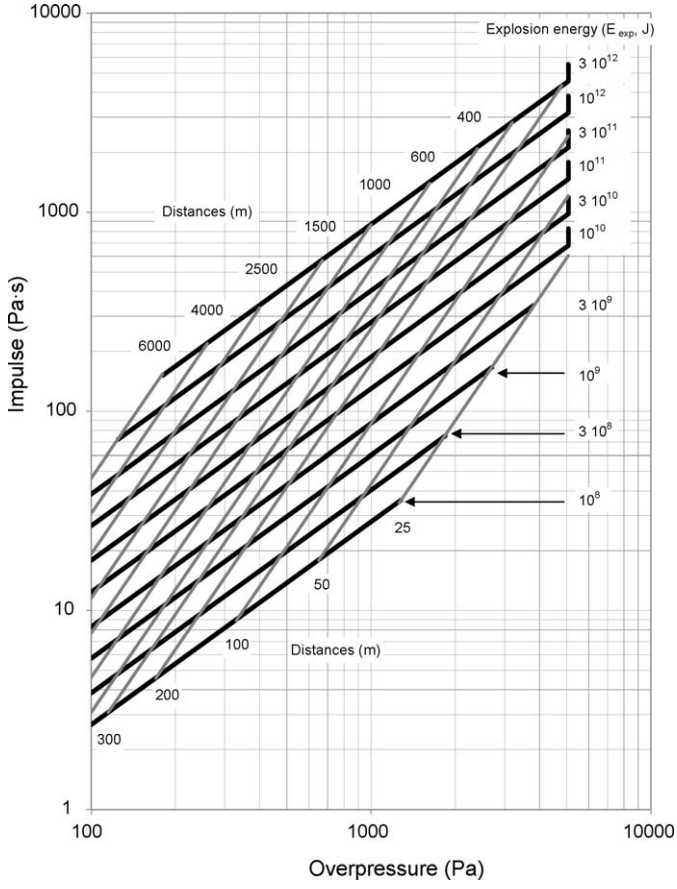

Fig. 5. *Characteristic* curves and *iso-distance* lines of VCEs with different energies and a charge strength of 3. Obtained using the TNO Multi-Energy model.

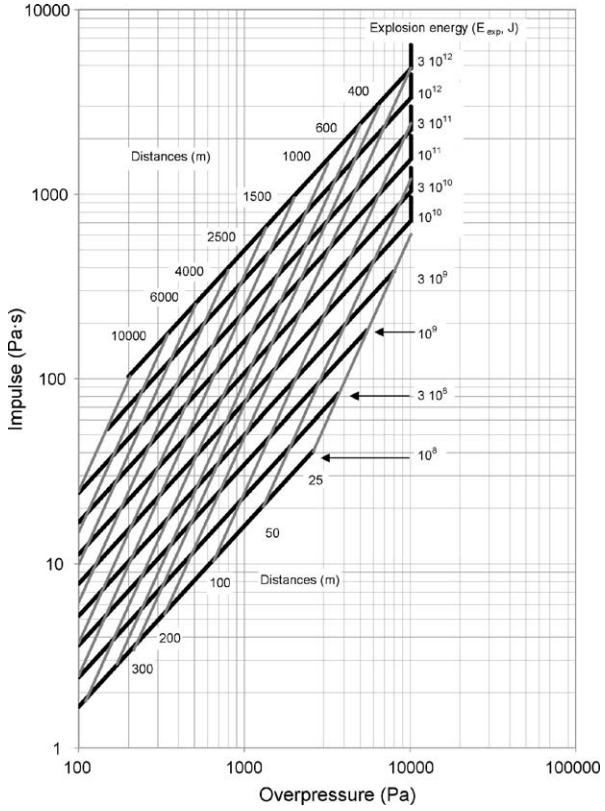

Fig. 6. *Characteristic* curves and *iso-distance* lines of VCEs with different energies and a charge strength of 4. Obtained using the TNO Multi-Energy model.

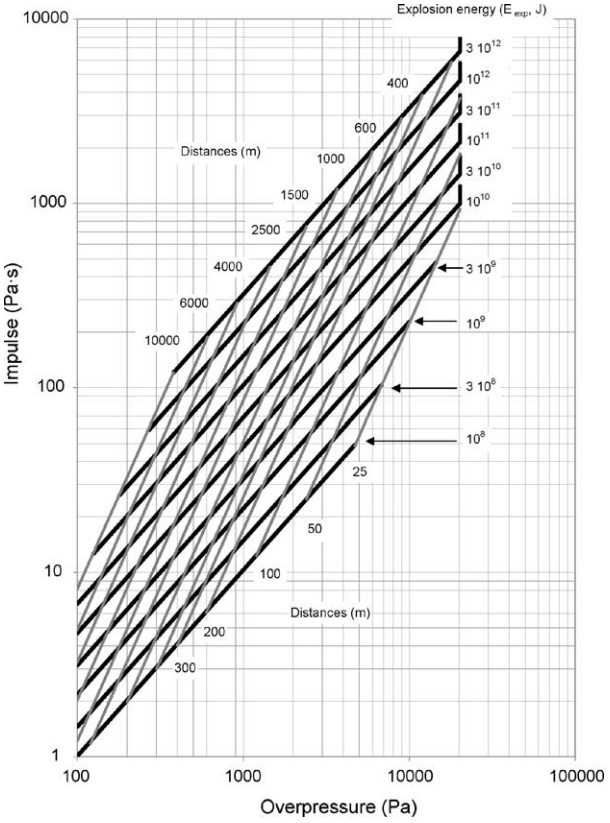

Fig. 7. *Characteristic* curves and *iso-distance* lines of VCEs with different energies and a charge strength of 5. Obtained using the TNO Multi-Energy model.

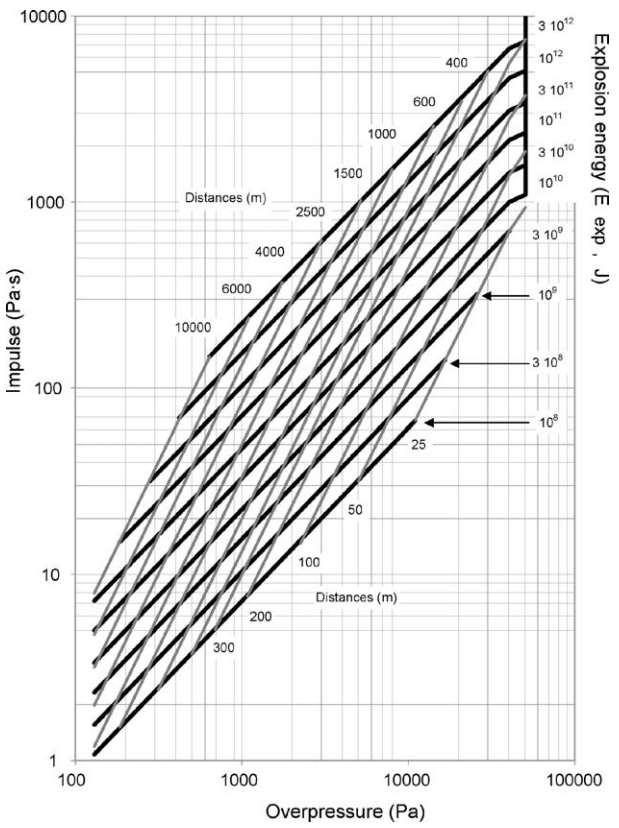

Fig. 8. *Characteristic* curves and *iso-distance* lines of VCEs with different energies and a charge strength of 6. Obtained using the TNO Multi-Energy model.

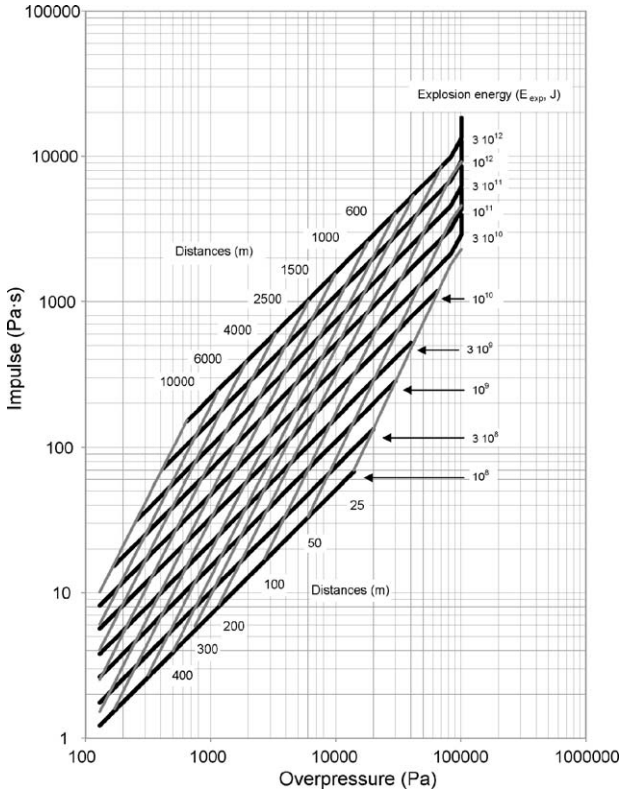

Fig. 9. *Characteristic* curves and *iso-distance* lines of VCEs with different energies and a charge strength of 7. Obtained using the TNO Multi-Energy model.

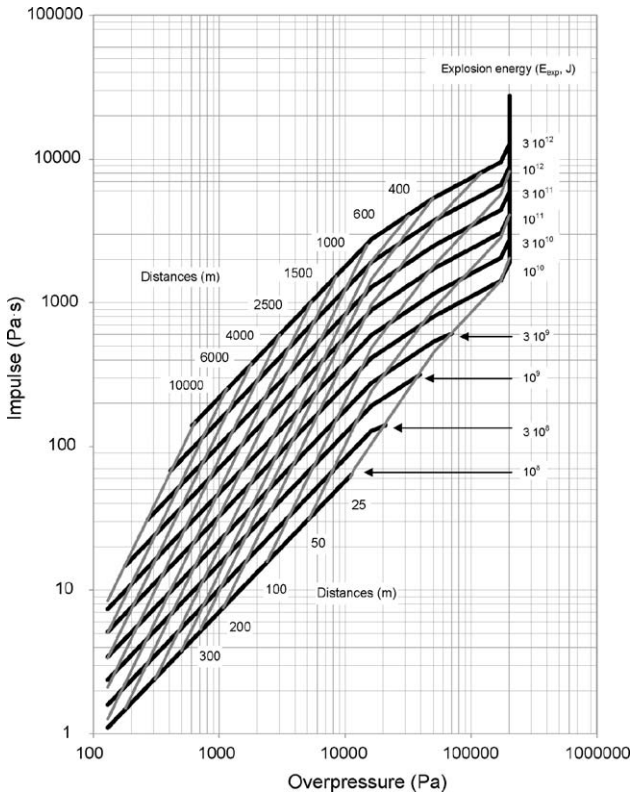

Fig. 10. *Characteristic* curves and *iso-distance* lines of VCEs with different energies and a charge strength of 8. Obtained using the TNO Multi-Energy model.

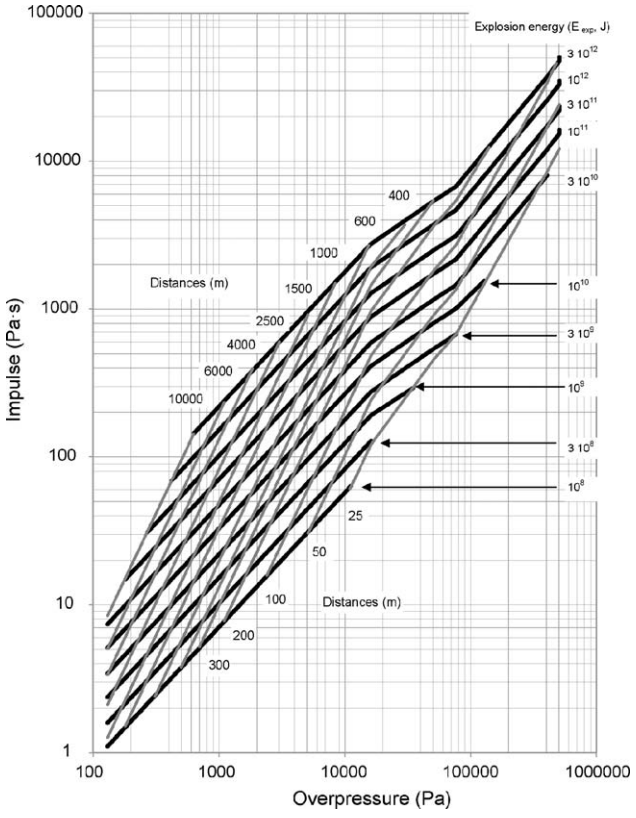

Fig. 11. *Characteristic* curves and *iso-distance* lines of VCEs with different energies and a charge strength of 9. Obtained using the TNO Multi-Energy model.

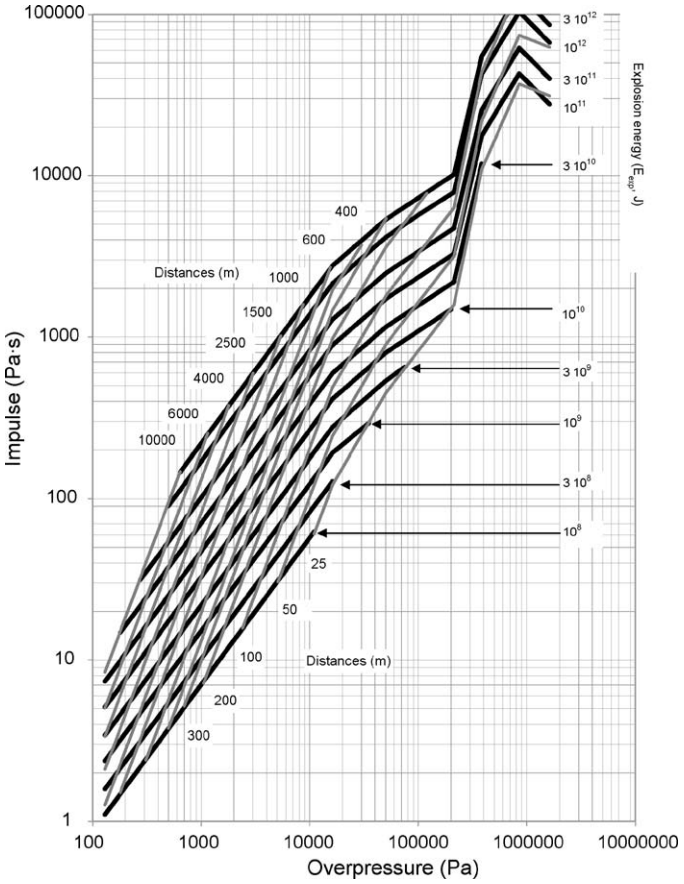

Fig. 12. *Characteristic* curves and *iso-distance* lines of VCEs with different energies and a charge strength of 10. Obtained using the TNO Multi-Energy model.

4. Conclusions

In an industrial accident caused by ignition of a vapour cloud, the TNO Multi-Energy model is often used to calculate overpressure and positive phase duration time from the released energy, and setting the explosion strength depending on the fuel involved and surrounding characteristics. From the model, the relationships between overpressure and impulse are obtained, depending on the explosion energy. Here, they are referred to as *characteristic* curves and, if represented in the same diagram, allow the determination of overpressure and impulse at each distance. Using *characteristic curves* simplifies the approach, as both overpressure and impulse can be determined in one step, avoiding any calculation of scaled magnitudes. This model, based on characteristic curves, allows an overview of the evolution and relationship of all variables involved in vapour cloud explosions. In summary, using this new methodology, simulation of explosions is simpler and faster.

References

[1] M.J. Tang, Q.A. Baker, A new set of blast curves from vapour cloud explosion, Process Safety Prog. 18 (3) (1999) 235–240.
[2] I. Chem. E (Institution of Chemical Engineers), Explosions in the Process Industries, Major Hazards Monograph. IChemE, UK, 1994.

[3] F.P. Lees, Loss prevention in the process industries, 2nd ed., Butterworth-Heinemann, London, 1996.
[4] S. Contini, G.F. Francocci, Rassegna di modelli per la valutazione degli effetti delle esplosioni negli impianti industriali. Centro Comune di Ricerca, Ispra, Italia. ISEI/IE 2397/93, 1993.
[5] S. Hoiset, B.H. Hjertager, T. Solberg, K.A. Malo, Flixborough revisited–an explosion simulation approach, J. Hazard. Mater. A77 (2000) 1–9.
[6] K. van Windergen, H.C. Salvesen, R. Perbal, Simulation of an accidental vapour cloud explosion, Process Safety Prog. 14 (3) (1995) 173–181.
[7] W.P.M. Mercx, A.C. van den Berg, Methods for the Calculation of Physical Effects (The Yellow book), TNO, The Netherlands, 1997.
[8] W.P.M. Mercx, A.C. van den Berg, C.J. Hayhurst, N.J. Robertson, K.C. Moran, Developments in vapour cloud explosion blast modelling, J. Hazard. Mater. 71 (2000) 301–319.
[9] R.P. Cleaver, C.G. Robinson, An analysis of the mechanisms of overpressure generation in vapour cloud explosions, J. Hazard. Mater. 45 (1996) 27–44.
[10] R.P. Cleaver, C.E. Humphreys, J.D. Morgan, C.G. Robinson, Development of a model to predict the effects of explosions in compact congested regions, J. Hazard. Mater. 53 (1997) 35–55.
[11] K.G. Kinsella, A rapid assesment methodology for the prediction of vapour cloud explosion overpressure, in: Proceedings of the International Conference and Exhibition on Safety, Health and Loss Prevention in the Oil, Chemical and Process Industries, Singapore, 1993.
[12] Q.A. Baker, M.J. Tang, E.A. Scheier, G.J. Silva, Vapour cloud explosion analysis, Process Safety Prog. 15 (2) (1996) 106–109.
[13] J.B.M.M. Eggen, GAME: Development of Guidance for the Application of the Multi-energy Method, TNO Prins Maurits Laboratory, Rijswijk, The Netherlands, 1998.
[14] W.P.M. Mercx, A.C. van den Berg, D. van Leeuwen, Application of correlations to quantify the source strength of vapour cloud explosions in realistic situations. Final report for the project: GAMES, TNO Prins Maurits Laboratory, Rijswijk, The Netherlands.
[15] J. Lobato, P. Cañizares, M. Rodrigo, C. Sáez, J. Linares, A comparison of hydrogen cloud explosion models and the study of the vulnerability of the damage caused by an explosion of H_2, Int. J. Hydrogen Energy 31 (2006) 1780–1790.
[16] J. Lobato, P. Cañizares, M. Rodrigo, C. Sáez, J. Linares, Study of the effects of an explosion of hydrogen in a lab, in: 2nd European Hydrogen Energy Conference, Zaragoza, November 2005, 2005, p. 646.
[17] F. Rigas, S. Sklavounos, Major hazards analysis for populations adjacent to chemical storage facilities, Process Safety Environ. Prot. 82 (B4) (2004) 1–11.
[18] M. Maremonti, G. Russo, E. Salzano, V. Tufano, Post-accident analysis of vapour cloud explosions in fuel storage areas, Process Safety Environ. Prot. 77 (B6) (1999) 360–365.
[19] F. Rigas, S. Sklavounos, Risk and consequence analyses of hazardous chemicals in marshalling yards and warehouses at Ikonio/Piraeus harbour, Greece, J. Loss Prevention Process Ind 15 (2002) 531–544.
[20] E. Salzano, V. Cozzani, The analysis of domino accidents triggered by vapor cloud explosions, Reliability Eng. System Safety 90 (2005) 271–284.